

# Chiral perturbation theory for electroweak reactions on deuterium

**Daniel R. Phillips**

Department of Physics and Astronomy, Ohio University, Athens, OH 45701, USA

**Abstract.** I summarize two recent applications of chiral perturbation theory to electromagnetic reactions on deuterium: elastic electron-deuteron scattering, and Compton scattering on deuterium. Both calculations have now been carried out to three orders in the chiral expansion. The expansion shows good convergence and is able to reproduce data for  $|\mathbf{q}| \lesssim 600$  MeV in  $ed$  and for  $\omega = 55\text{--}95$  MeV in  $\gamma d$ . These results demonstrate that  $\chi$ PT can be used to reliably compute operators and wave functions for low-momentum-transfer reactions in light nuclear systems.

## 1. Introduction

In recent years effective field theory (EFT) techniques have found increasing acceptance in nuclear physics. EFT facilitates the systematic separation of the effects of high-momentum physics from those of low-momentum physics. In nuclear physics there are many different momentum scales present. But for the  $A = 2$  system the key ones would seem to be:

$$\sqrt{MB} \ll m_\pi \ll \Lambda_{\chi\text{SB}}, \quad (1)$$

with  $B$  the binding energy of deuterium,  $m_\pi$  and  $M$  the pion and nucleon masses, and  $\Lambda_{\chi\text{SB}}$  the scale of chiral-symmetry breaking, which is of the order of the mass of the  $\rho$  meson. An EFT based on the first hierarchy— $\sqrt{MB} \ll m_\pi$ —has had considerable success describing very-low-energy reactions in  $A = 2$  and  $A = 3$  (for reviews see [1, 2, 3]), and has recently been extended to  $A = 4$  [4]. Here I will focus on the EFT built on the second hierarchy— $m_\pi \ll \Lambda_{\chi\text{SB}}$ . This EFT is chiral perturbation theory ( $\chi$ PT) (for a review see [5]). Here the low-momentum physics is described by a quantum field theory of nucleons and pions whose Lagrangian is the most general one that respects the approximate chiral symmetry of QCD and the pattern of its breaking. Higher-energy effects of QCD appear in  $\chi$ PT as non-renormalizable contact operators. Any process involving nucleons and an arbitrary number of (soft) pions and photons should then be computable as an expansion in the ratio of nucleon or probe momenta (denoted here by  $p$  and  $q$ ) and  $m_\pi$  to  $\Lambda_{\chi\text{SB}}$ .

Since typical momenta in light nuclei are  $\lesssim m_\pi$  we would expect to be able to calculate the response of such nuclei to low-momentum electroweak probes using  $\chi$ PT.

As we will see below,  $\chi$ PT provides a systematic way to compute what in nuclear-structure physics would be called “bare operators”. But the operators computed in this fashion include pieces which account for the fact that they are not actually “bare” if one thinks about the physics at scale  $\Lambda_{\chi\text{SB}}$  which has been “integrated out” of the low-momentum theory of nucleons and pions: high-momentum nucleon modes, the delta isobar, mesons such as the rho, pomerons, M-branes, etc.

Here I will argue that these operators produce results for electromagnetic few-nucleon reactions which are model independent, can be systematically improved by going to higher order, and yield a good description of the data over the region of validity of the EFT. Section 2 outlines the  $\chi$ PT expansion, and briefly discusses how to obtain deuteron wave functions using it. Section 3 then looks at electron-deuteron scattering in  $\chi$ PT as a probe of deuteron structure. Section 4 examines the use of Compton scattering on the deuteron—in particular as a way to extract isoscalar polarizabilities of the nucleon.

## 2. Power counting and deuteron wave functions

### 2.1. Power counting

Consider an elastic scattering process on the deuteron. If  $\hat{O}$  is the transition operator for this reaction then the amplitude in question is simply  $\langle\psi|\hat{O}|\psi\rangle$ , with  $|\psi\rangle$  the deuteron wave function. In this section, we follow Weinberg [6], and divide the formulation of a systematic expansion for this amplitude into two parts: the expansion for  $\hat{O}$ , and the construction of  $|\psi\rangle$ .

Chiral perturbation theory gives a systematic expansion for  $\hat{O}$  of the form

$$\hat{O} = \sum_{n=0}^{\infty} \hat{O}^{(n)}, \quad (2)$$

where we have labeled the contributions to  $\hat{O}$  by their order  $n$  in the small parameter  $P \equiv p/\Lambda_{\chi\text{SB}}, q/\Lambda_{\chi\text{SB}}, m_{\pi}/\Lambda_{\chi\text{SB}}$ .

To construct  $\hat{O}^{(n)}$  one first writes down the vertices appearing in the chiral Lagrangian up to order  $n$ . One then draws all of the two-body, two-nucleon-irreducible, Feynman graphs for the process of interest which are of chiral order  $P^n$ . The rules for calculating the chiral order of a particular graph are:

- Each nucleon propagator scales like  $1/P$  (provided that the energy flowing through the nucleon line is  $\sim m_{\pi}$ );
- Each loop contributes  $P^4$ ;
- Graphs in which both particles participate in the reaction acquire a factor of  $P^3$ ;
- Each pion propagator scales like  $1/P^2$ ;
- Each vertex from the  $n$ th-order piece of the chiral Lagrangian contributes  $P^n$ .

In consequence more complicated contributions involving two-body mechanisms, and/or higher-order vertices, and/or more loops are suppressed by powers of  $P$ .

## 2.2. Deuteron wave functions

This leaves us with the problem of constructing a deuteron wave function that is consistent with the operator  $\hat{O}$ . Weinberg's proposal was to use the  $\chi$ PT expansion (2) for the  $NN$  potential  $V$ , and then solve the Schrödinger equation to find the deuteron (or other nuclear) wave function [6]. Matrix elements  $\langle\psi|\hat{O}|\psi\rangle$  should then incorporate the consequences of chiral-symmetry breaking in a model-independent way.

Calculations have shown that the  $NN$  phase shifts can be understood, and deuteron bound-state static properties reliably computed, with  $NN$  potentials derived from  $\chi$ PT [7, 8, 9, 10, 11]. This is now a sophisticated enterprise, with N<sup>3</sup>LO [ $\mathcal{O}(P^4)$ ] potentials recently having been obtained [11, 12, 13]. These potentials can reproduce  $NN$  data with an accuracy which rivals that of “high-quality”  $NN$  potentials, at least for  $T_{\text{lab}} < 200$  MeV.

In the Goldstone-boson and single-nucleon sector  $\chi$ PT works because loop effects are generically suppressed by powers of the small parameter  $P$ . In zero and one-nucleon reactions the power counting in  $P$  applies to the amplitude, and not to the two-particle potential. However, the existence of nuclei tells us immediately that a power counting in which all loop effects are suppressed cannot be correct for the multi-nucleon case, since if it were there would be no nuclei, and neither we, or this workshop, would occur. Weinberg's proposal to instead power-count the potential is one response to this dilemma. However, its consistency has been vigorously debated in the literature (see [1, 2, 3] for reviews). Beane *et al.* [14] have shown that Weinberg's proposal is consistent to leading order in the  ${}^3S_1 - {}^3D_1$  channel, but there remain questions about the consistency in other channels and at higher orders [15, 16]. Here we will use wave functions calculated according to the Weinberg proposal. One of our objectives will be to assess whether such a procedure really does lead to convergent EFT expansions for the processes under consideration, or whether problems along the lines of those raised in Refs. [15, 16] also occur in the chiral EFT for electroweak reactions on deuterium.

## 3. Elastic electron scattering on deuterium

One quantitative test of  $\chi$ PT's deuteron wave functions is provided by elastic electron-deuteron scattering. We thus turn our attention to the deuteron electromagnetic form factors  $G_C$ ,  $G_Q$ , and  $G_M$ . These are matrix elements of the deuteron current  $J_\mu$ , with:

$$G_C = \frac{1}{3|e|} \left( \langle 1 | J^0 | 1 \rangle + \langle 0 | J^0 | 0 \rangle + \langle -1 | J^0 | -1 \rangle \right), \quad (3)$$

$$G_Q = \frac{1}{2|e|\eta M_d^2} \left( \langle 0 | J^0 | 0 \rangle - \langle 1 | J^0 | 1 \rangle \right), \quad G_M = -\frac{1}{\sqrt{2}\eta|e|} \langle 1 | J^+ | 0 \rangle, \quad (4)$$

where we have labeled these (non-relativistic) deuteron states by the projection of the deuteron spin along the direction of the momentum transfer  $\mathbf{q}$  and  $\eta \equiv |\mathbf{q}|^2/(4M_d^2)$ .  $G_C$ ,  $G_Q$ , and  $G_M$  are related to the experimentally-measured  $A$ ,  $B$ , and  $T_{20}$  in the usual way, with  $T_{20}$  being primarily sensitive to  $G_Q/G_C$  and  $B$  depending only to  $G_M$ . Here we will compare calculations of the charge and quadrupole form factor with the recent extractions of  $G_C$  and  $G_Q$  from data [17].

Both of these form factors involve the zeroth-component of the deuteron four-current  $J^0$ . Here we split  $J^0$  into two pieces: a one-body part, and a two-body part. The one-body part of  $J^0$  begins at order  $|e|$  (the proton charge) with the impulse approximation diagram calculated with the non-relativistic single-nucleon charge operator for structureless nucleons. Corrections to the single-nucleon charge operator from relativistic effects and nucleon sub-structure are suppressed by two powers of  $P$ , and thus arise at  $O(eP^2)$ , which is the next-to-leading order (NLO) for  $G_C$  and  $G_Q$ . At this order one might also expect meson-exchange current (MEC) contributions. However, all MECs constructed with vertices from  $\mathcal{L}_{\pi N}^{(1)}$  are isovector. These play a role in, e.g.  $np \rightarrow d\gamma$  [18]. The first MEC effect in  $ed \rightarrow ed$  does not occur until N<sup>2</sup>LO, or  $O(eP^3)$ , where an  $NN\pi\gamma$  vertex from  $\mathcal{L}_{\pi N}^{(2)}$  gets included in an isoscalar two-body contribution to the deuteron charge operator (see Fig. 1(b)) ‡.

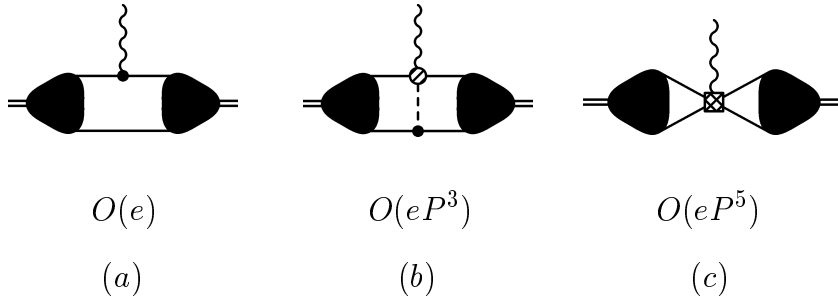


**Figure 1.** Diagrams representing the leading contribution to  $J_0$  [(a)], the leading two-body contribution [(b)], and the dominant short-distance piece [(c)]. Solid circles are vertices from  $\mathcal{L}_{\pi N}^{(1)}$ , and the shaded circle is the vertex from  $\mathcal{L}_{\pi N}^{(2)}$ .

The most important correction that arises at NLO is the inclusion of *nucleon* sub-structure. At  $O(eP^2)$  the isoscalar nucleon form factors are dominated by short-distance physics, and so the only correction to the point-like leading-order result comes from the inclusion of the nucleon’s electric radius. For the isoscalar combination of nucleon electric form factors  $\chi$ PT to  $O(eP^2)$  gives:

$$G_E^{(s)} \chi_{\text{PT NLO}} = 1 - \frac{1}{6} \langle r_E^{(s)2} \rangle q^2. \quad (5)$$

This description of nucleon structure breaks down at momentum transfers  $q$  of order 300 MeV. There is a concomitant failure in the description of  $ed$  scattering data [20, 21]. In order to focus on *deuteron* structure, in the results presented below I have chosen to circumvent this issue by using a “factorized” inclusion of nucleon structure [21]:  $\chi$ PT is used to compute the ratio  $\frac{G_C}{G_E^{(s)}}$ . This allows us to use experimentally-measured single-nucleon form factors § in the calculation, thereby allowing us to test how far the theory is able to describe the  $NN$  dynamics.

‡ This exchange-charge contribution was first derived by Riska [19].

§ There is a bit of an issue of circularity here, since  $ed$  scattering data is one input to the extraction of the neutron electric form factor.

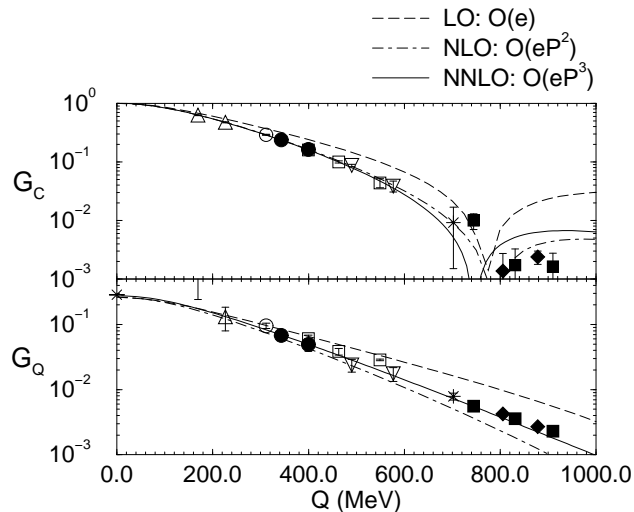


**Figure 2.** The deuteron charge and quadrupole form factors to NNLO in chiral perturbation theory. The experimental data is taken from the compilation of Ref. [17].  $G_Q$  is in units of  $\text{fm}^2$ .

The results for  $G_C$  and  $G_Q$  are shown in Fig. 2. The figure demonstrates that convergence is quite good below  $q \sim 700$  MeV. The results shown are for the NLO chiral wave function. It is clear that—provided information from single-nucleon form factors is taken into account— $\chi$ PT is perfectly capable of describing the charge and quadrupole form factors of deuterium at least as far as the minimum in  $G_C$ .

$G_M$  can be obtained in a similar way. The LO contribution to  $G_M$  is  $O(eP)$ . The first two-body mechanisms enter at  $O(eP^4)$ , when an undetermined two-body counterterm, as well as a long-range two-body current with an undetermined coefficient, appear [20, 22]. Results for  $G_M$  at  $O(eP^3)$  turn out to be of similar quality to those for  $G_C$  [21], but are somewhat more sensitive to short-distance physics, as expected given the presence of a counterterm at NNLO in this observable.

Using the NNLO chiral wave function, high-quality potential-model wave functions, or indeed simple wave functions which include only one-pion exchange regulated by a square well at short distances, does not modify the plots for  $G_C$  and  $G_Q$  greatly below  $q = 700$  MeV [21]. As long as wave functions with the same long-distance parts are employed these observables are apparently not very sensitive to the choice of  $|\psi\rangle$ . In the language of the no-core shell model they do not “renormalize strongly”. (An important exception is the deuteron quadrupole moment,  $Q_d$ .) This is good news for Weinberg’s power counting, because the first operators with which  $J_0$  can be renormalized occur at  $O(eP^5)$  (Fig. 1(c)). Therefore it was to be expected that operator renormalization would have this small impact on  $G_C$  and  $G_Q$ . Furthermore, the dominant piece of the operator renormalization can be taken into account by adjusting the coefficients of the  $O(eP^5)$  operators to reproduce, e.g.  $\langle r_d^2 \rangle$  and  $Q_d$ . This would then push the omitted effects of operator renormalization in these observables to  $O(eP^7)$ .

#### 4. Compton scattering on deuterium

Compton scattering on the nucleon at low energies is a fundamental probe of the long-distance structure of these hadrons. This process has been studied in  $\chi PT$  in [23, 24]. The following results for the proton polarizabilities were obtained at  $O(e^2P)$ :

$$\alpha_p = \frac{5e^2g_A^2}{384\pi^2f_\pi^2m_\pi} = 12.2 \times 10^{-4} \text{ fm}^3, \quad \beta_p = \frac{1}{10}\alpha_p = 1.2 \times 10^{-4} \text{ fm}^3. \quad (6)$$

Going to next order in the chiral expansion single-nucleon counterterms which shift the polarizabilities enter the calculation. Using the  $\gamma p$  amplitude computed by McGovern to  $O(e^2P^2)$  [25] we fitted  $\gamma p$  data over the kinematic range  $\omega, \sqrt{|t|} < 180$  MeV [26].

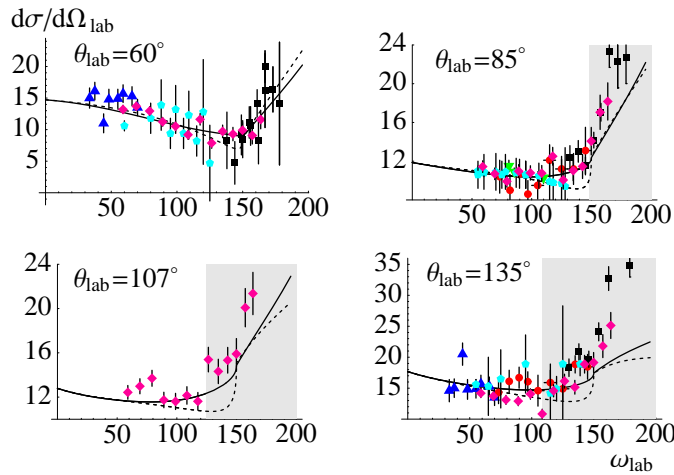


**Figure 3.** Results of the  $O(e^2P^2)$  EFT best fit to the differential cross sections for Compton scattering on the proton at various angles, compared to the experimental data from various facilities. The gray region is excluded from the fit. References for the data and a legend for the symbols are given in Ref. [25].

The best fit for the proton electric and magnetic polarizabilities is

$$\alpha_p = (12.1 \pm 1.1)_{-0.5}^{+0.5} \times 10^{-4} \text{ fm}^3, \quad \beta_p = (3.4 \pm 1.1)_{-0.1}^{+0.1} \times 10^{-4} \text{ fm}^3. \quad (7)$$

Statistical ( $1-\sigma$ ) errors are inside the brackets. An estimate of the theoretical error due to truncation of the expansion at  $O(e^2P^2)$  is given outside the brackets. The result (7) is compatible with other extractions, although the central value of  $\beta_p$  is higher [27].

One would like to perform a similar analysis for  $\gamma d$  scattering data. Coherent Compton scattering on a deuteron target has been measured at  $E_\gamma = 49$  and 69 MeV by the Illinois group [28], at  $E_\gamma = 84.2 - 104.5$  MeV at Saskatoon [29], and at  $E_\gamma = 55$  and 66 MeV at MAXlab at Lund [30]. Such data should permit an extraction of the isoscalar nucleon polarizabilities  $\alpha_N$  and  $\beta_N$ . These are interesting, not only as fundamental nucleon-structure parameters, but also because  $\chi PT$  predicts  $\alpha_N = \alpha_p$ ,  $\beta_N = \beta_p$  at  $O(e^2P)$ . The amplitude for  $\gamma d$  scattering involves mechanisms other than Compton scattering on the individual constituent nucleons. So, our desire to extract nucleon polarizabilities argues for a theoretical calculation of this reaction that is under control in the sense that it accounts for *all* mechanisms to a given order in  $\chi PT$ .

The Compton amplitude we wish to evaluate is (in the  $\gamma d$  center-of-mass frame):

$$T_{M'\lambda'M\lambda}^{\gamma d}(\vec{k}', \vec{k}) = \int \frac{d^3 p}{(2\pi)^3} \psi_{M'}\left(\vec{p} + \frac{\vec{k} - \vec{k}'}{2}\right) T_{\gamma N_{\lambda'\lambda}}(\vec{k}', \vec{k}) \psi_M(\vec{p}) + \int \frac{d^3 p d^3 p'}{(2\pi)^6} \psi_{M'}(\vec{p}') T_{\gamma NN_{\lambda'\lambda}}^{2N}(\vec{k}', \vec{k}) \psi_M(\vec{p}) \quad (8)$$

where  $M$  ( $M'$ ) is the initial (final) deuteron spin state, and  $\lambda$  ( $\lambda'$ ) is the initial (final) photon polarization state, and  $\vec{k}$  ( $\vec{k}'$ ) the initial (final) photon three-momentum, which are constrained to  $|\vec{k}| = |\vec{k}'| = \omega$ . The first integral is represented by the graphs of Fig. 4 where the photon interacts with only one nucleon. The second integral corresponds to the graphs of Fig. 5 where the current is of a two-body nature.

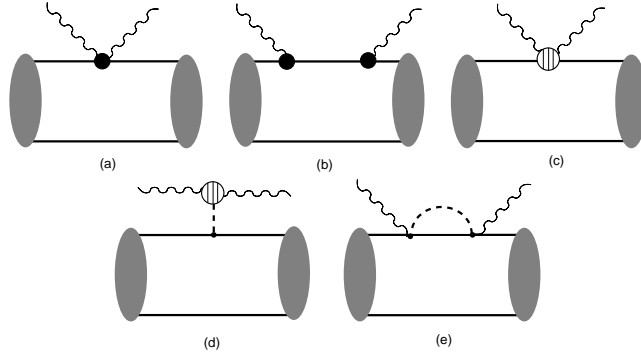


**Figure 4.** Graphs which contribute to Compton scattering on the deuteron at  $\mathcal{O}(e^2)$  (a) and  $\mathcal{O}(e^2 P)$  (b-e). The sliced blob in graph (c) is from  $\mathcal{L}_{\pi N}^{(3)}$ . Crossed graphs are not shown.

The LO contribution to Compton scattering on the deuteron is shown in Fig. 4(a). This graph involves a vertex from  $\mathcal{L}_{\pi N}^{(2)}$  and so is  $\mathcal{O}(e^2)$ . This contribution is simply the Thomson term for scattering on the proton. There is thus no sensitivity to either two-body contributions *or* nucleon polarizabilities at this order. At  $\mathcal{O}(e^2 P)$  there are several more graphs with a spectator nucleon (Figs. 4(b),(c),(d)), as well as graphs involving an exchanged pion with leading order vertices (Fig. 5) and one-loop graphs with a spectator nucleon (Fig. 4(e)) [31]. Graphs such as Fig. 4(e) contain the physics of the proton and neutron polarizabilities at  $\mathcal{O}(e^2 P)$  in  $\chi$ PT.

We employed a variety of wave functions  $|\psi\rangle$ , and found moderate wave-function sensitivity. Results shown here are generated with the NLO chiral wave function of Ref. [9]. Fig. 6 shows the results of a fit to the world's modern  $\gamma d$  data. The dotted line is the prediction at  $\mathcal{O}(e^2)$  in the kernel, where the second contribution in Eq. (8) is zero, and the single-scattering contribution is given solely by Fig. 4(a). It is quite remarkable how well the  $\mathcal{O}(e^2)$  calculation reproduces the 49 MeV data. However, the agreement is somewhat serendipitous: there are significant  $\mathcal{O}(e^2 P)$  corrections. At these lower photon energies Weinberg power counting begins to break down, since it is designed for  $\omega \sim m_\pi$ , and does *not* recover the deuteron Thomson amplitude as  $\omega \rightarrow 0$ . Correcting the power counting to remedy this difficulty appears to improve the description of the 49 MeV data, without significantly modifying the higher-energy results [26, 31].

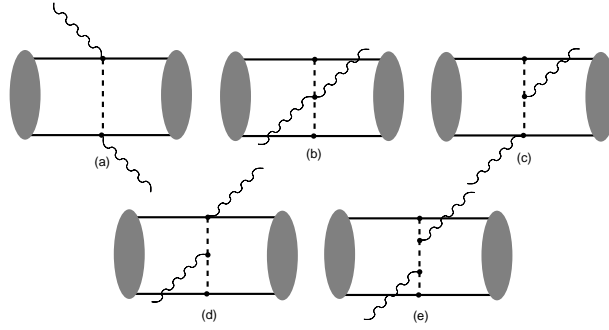


**Figure 5.** Two-body graphs which contribute to  $\gamma d$  scattering at  $O(e^2P)$ . Crossed graphs are not shown.

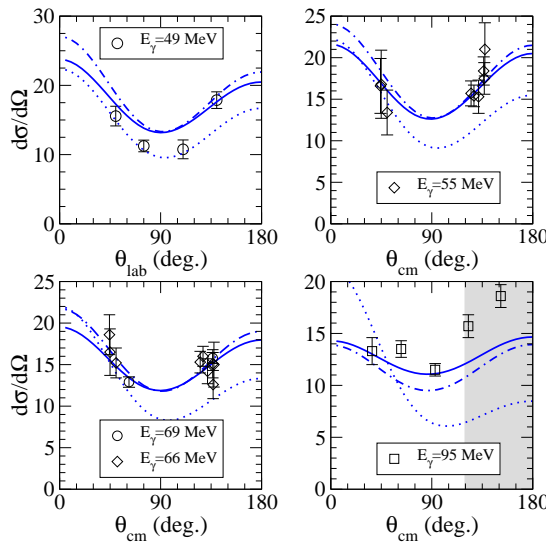


**Figure 6.** Results of the  $O(e^2)$  (dotted),  $O(e^2P)$  (dashed), and  $O(e^2P^2)$  (solid) calculations for  $\gamma d$  scattering as compared to data at  $E_\gamma = 49$  MeV [28], 55 MeV [30], 66 & 69 MeV [28, 30], and 95 MeV [29]. Only statistical errors on the data are shown. The gray region is excluded from the fit.

At  $O(e^2P)$  all contributions to the kernel are fixed in terms of known pion and nucleon parameters, so to this order  $\chi PT$  makes *predictions* for deuteron Compton scattering. Note that the  $O(e^2P)$  corrections get larger as  $\omega$  is increased—as expected. The agreement of the  $O(e^2P)$  calculation with the intermediate-energy data sets is very good, although only limited conclusions can be drawn. These results are not very different from other, potential-model, calculations [32, 33, 34].

At  $O(e^2P^2)$  terms enter the single-nucleon amplitude which allow us to fit  $\alpha_N$  and  $\beta_N$  to  $\gamma d$  data. A number of new two-body currents also appear. However, there are still no short-distance  $\gamma NN$  operators contributing to  $\gamma d$  scattering at this order. Therefore an  $O(e^2P^2)$  calculation allows us to test the single-nucleon physics which is used to predict the results of coherent scattering on deuterium, since there are no undetermined parameters in the two-body mechanisms that enter.



Unfortunately the data is fairly sparse, and the sensitivity to the  $NN$  wave function quite large, so our fit does not tie down  $\alpha_N$  and  $\beta_N$  very accurately. The result is:

$$\alpha_N = (13.0 \pm 1.9)_{-1.5}^{+3.9} \times 10^{-4} \text{ fm}^3, \quad \beta_N = (-1.8 \pm 1.9)_{-0.9}^{+2.1} \times 10^{-4} \text{ fm}^3. \quad (9)$$

The errors inside the brackets are statistical and those outside are an estimate of the effect from higher-order terms. (For details see Ref. [26].) The fit only includes data satisfying  $\omega, \sqrt{|t|} < 160$  MeV. Recent work suggests that to describe the backward-angle points at 95 MeV requires the inclusion of an explicit delta degree of freedom [35].

The second error quoted on  $\alpha_N$  and  $\beta_N$  is large because, as alluded to above, cross sections depend on the choice of  $|\psi\rangle$  at the 10–20% level. This change in the  $\gamma d$  cross section has a sizable impact on the extraction of  $\alpha_N$  and  $\beta_N$ . While not all of the wave functions we employed are consistent with  $\chi$ PT, they do all have the correct long-distance behavior. The differences we see are thus a consequence of different short-range behavior in, say, the Nijm93 and NLO  $\chi$ PT  $NN$  potentials. As such they should be renormalized by  $\gamma NN$  contact operators. However, Weinberg power counting predicts that the operators which do this do not appear until (at least)  $O(e^2 P^3)$ . Thus the degree of variability seen in our results with different wave functions could be viewed as inconsistent with this power counting. Indeed, it may be necessary to modify the power counting so that, e.g.  $\gamma NN$  contact operators appear at a lower order than is indicated by the naive  $\chi$ PT power counting we have used for  $\hat{O}$ . The issue here is one of relevance to nuclear-structure physics: it speaks of the need to properly renormalize the effective  $\gamma NN$  operators found when high-energy degrees of freedom are integrated out of our EFT of the  $NN$  system. Further understanding of this issue is also crucial if  $\chi$ PT is to be an accurate calculational tool for low-energy reactions on deuterium.

## 5. I thought you said electro $weak$ ?

There is nothing in what I have presented so far that is particular to the photon as a probe. Analogous expansions can be made for axial currents. The result is a systematic approach to reactions such as  $pp \rightarrow d + e^+ + \nu_e$  and  $\nu d \rightarrow \nu d$ . I do not have room to properly describe the beautiful work on these reactions by Park, Ando, and collaborators [36, 37]. In my view a particular strength of that work is the application of the same  $\chi$ PT electroweak operators to  $A = 2, 3$ , and 4. Ref. [36] uses the well-known tritium beta decay rate to fix the strength of an (otherwise poorly constrained) two-body contribution to the Gamow-Teller transition operator. This renormalizes the effective  $NN$  Gamow-Teller operator to such high accuracy that the  $pp$ -fusion  $S$  factor has an estimated error from higher-order terms of less than 0.5%. The same one- and two-nucleon operators are then used to predict the reaction  $p + {}^3\text{He} \rightarrow {}^4\text{He} + e^+ + \nu_e$  [36] and  $\nu d$  scattering [37]. This is a great example of  $\chi$ PT's ability to give a systematic derivation of electroweak operators that can be used in a variety of light nuclear systems to yield accurate predictions.

## Acknowledgments

I thank the organizers of the ‘Workshop on Microscopic Nuclear Structure Theory’ for their invitation to participate in a stimulating and timely meeting. I am also grateful to Silas Beane, Manuel Malheiro, Judith McGovern, and Bira van Kolck for a profitable and enjoyable collaboration.

## References

- [1] van Kolck, U., *Prog. Part. Nucl. Phys.*, **43**, 409 (1999).
- [2] Beane, S. R., Bedaque, P. F., Haxton, W., Phillips, D. R., and Savage, M. J., in *At the frontier of particle physics—Handbook of QCD*, M. Shifman, ed. (World Scientific, Singapore, 2000).
- [3] Bedaque, P. F. and van Kolck, U., *Ann. Rev. Nucl. Part. Sci.*, **52**, 339 (2002).
- [4] Hammer, H.-W., *these proceedings*.
- [5] Bernard, V., Kaiser, N., and Meißner, U.-G., *Int. Jour. of Mod. Phys. E*, **4**, 193 (1995).
- [6] Weinberg, S., *Phys. Lett.*, **B251**, 288 (1990); *ibid.*, **B295**, 114 (1992); *Nucl. Phys.*, **B363**, 3 (1991).
- [7] Ordonéz, C., Ray, L., and van Kolck, U., *Phys. Rev. C*, **53**, 2086 (1996).
- [8] Kaiser, N., Brockmann, R., and Weise, W., *Nucl. Phys.*, **A625**, 758 (1997).
- [9] Epelbaum, E., Glöckle, W., and Meißner, U.-G., *Nucl. Phys.*, **A671**, 295 (1999).
- [10] Rentmeester, M. C. M., Timmermans, R. G. E., Friar, J. L., and de Swart, J. J., *Phys. Rev. Lett.*, **82**, 4992 (1999).
- [11] Entem, D. R., and Machleidt, R., *Phys. Rev. C*, **68**, 041001 (2003).
- [12] Epelbaum, E., Glöckle, W., and Meißner, U.-G., arXiv:nucl-th/0405048.
- [13] Machleidt, R., *these proceedings*.
- [14] Beane, S. R., Bedaque, P. F., Savage, M. J., and van Kolck, U., *Nucl. Phys.*, **A700**, 377 (2002).
- [15] Kaplan, D. B., Savage, M. J., and Wise, M. B., *Nucl. Phys.*, **B478**, 629 (1996).
- [16] Nogga, A., Timmermans, R., van Kolck, U., *Private communication*.
- [17] Abbott, D., et al. [JLAB t20 Collaboration] *Eur. Phys. J.*, **A7**, 421 (2000).
- [18] Park, T.-S., Min, D.-P., and Rho, M., *Nucl. Phys.*, **A596**, 515 (1996).
- [19] Riska, D. O., *Prog. Part. Nucl. Phys.*, **11**, 199 (1984).
- [20] Meißner, U.-G., and Walzl, M., *Phys. Lett.*, **B513**, 37 (2001).
- [21] Phillips, D. R., *Phys. Lett.*, **B567**, 12 (2003).
- [22] Park, T.-S., Kubodera, K., Min, D.-P., and Rho, M., *Phys. Lett.*, **B472**, 232 (2000).
- [23] Bernard, V., Kaiser, N., and Meißner, U. G., *Nucl. Phys.*, **B383**, 442–496 (1992).
- [24] Bernard, V., Kaiser, N., Kambor, J., and Meißner, U. G., *Nucl. Phys.*, **B388**, 315–345 (1992).
- [25] McGovern, J., *Phys. Rev. C*, **63**, 064608 (2001).
- [26] Beane, S. R., Malheiro, M., McGovern, J. A., Phillips, D. R., and van Kolck, U., *Phys. Lett.*, **B567**, 200 (2003), erratum *ibid.*, **B607**, 320 (2005); *Nucl. Phys.*, **A747**, 311 (2005).
- [27] Groom, D. E., et al. [Particle Data Group], *Eur. Phys. J. C*, **15**, 1 (2000).
- [28] Lucas, M. A., Ph.D. thesis, University of Illinois (1994), unpublished.
- [29] Hornidge, D. L., et al., *Phys. Rev. Lett.*, **84**, 2334 (2000).
- [30] Lundin, M., et al., *Phys. Rev. Lett.*, **90**, 192501 (2003).
- [31] Beane, S. R., Malheiro, M., Phillips, D. R., and van Kolck, U., *Nucl. Phys.*, **A656**, 367 (1999).
- [32] Wilbois, T., Wilhelm, P., and Arenhövel, H., *Few Bod. Sys.*, **9**, 263 (1995).
- [33] Levchuk, M. I., and L’vov, A. I., *Nucl. Phys.*, **A674**, 449 (2000).
- [34] Karakowski, J. J., and Miller, G. A., *Phys. Rev. C*, **60**, 014001 (1999).
- [35] Hildebrandt, R., Griebhammer, H., Hemmert, T., Phillips, D., *Nucl. Phys.*, **A748**, 573 (2005).
- [36] Park, T. S., et al. *Phys. Rev. C*, **67**, 055206 (2003).
- [37] Ando, S., Song, Y. H., Park, T. S., Fearing, H. W., and Kubodera, K., *Phys. Lett.* **B555**, 49 (2003).